Chemical Science

Accepted Manuscript

This article can be cited before page numbers have been issued, to do this please use: Z. Zheng, W. Geng, J. Gao, Y. Wang, H. W. Sun and D. Guo, *Chem. Sci.*, 2018, DOI: 10.1039/C7SC04989G.

ROYAL SOCIETY OF CHEMISTRY

rsc.li/chemical-science

View Article Online
DOI: 10.1039/C7SC04989G

Journal Name

ARTICLE

Ultrasensitive and Specific Fluorescence Detection of a Cancer Biomarker via Nanomolar Binding to a Guanidinium-modified Calixarene†

Received 00th January 20xx,
Accepted 00th January 20xx

DOI: 10.1039/x0xx00000x

www.rsc.org/

Zhe Zheng,[a] Wen-Chao Geng,[a] Jie Gao,[a] Yu-Ying Wang,[a] Hongwei Sun[a] and Dong-Sheng Guo*[a,b]

We design a water-soluble guanidinium-modified calix[5]arene to target lysophosphatidic acid (LPA), an ideal biomarker for early diagnosis of ovarian and other gynecologic cancers, achieving binding on the nanomolar level. Indicator displacement assay, coupled with differential sensing, enables ultrasensitive and specific detection of LPA. Moreover, we show that, using a calibration line, the LPA concentration in untreated serum can be quantified in the biologically relevant low μM range with a detection limit of 1.7 μM. The reported approach exhibits feasible application in diagnosing ovarian and other gynecologic cancers, especially at their early stages.

Introduction

Quantitatively detecting cancer biomarkers, especially those non-invasive in plasma, is of great importance for early diagnosis, which facilitates effective treatment and improves the survival rate of cancer patients.[1] Lysophosphatidic acid (LPA), one kind of bioactive phospholipids, is an ideal biomarker for the early detection of ovarian and other gynecologic cancers.[2] The LPA concentrations in healthy human plasma are approximately 0.1–6.3 μM and the danger levels of LPA for gynecologic cancers are indicated by concentrations on the order of 63.2 μM.[3] The routine diagnostic testing of plasma LPA level is limited by present detect techniques, such as tandem mass spectroscopy, capillary electrophoresis and radio-enzymatic assays,[4] which need sophisticated devices and complicated procedures. Optical methods (via fluorescence or colorimetric changes) represent powerful sensing modalities due to their low cost, ease of use and high sensitivity.[5] Up to now, there are several examples of detecting LPA by optical methods, but they generally suffered from drawbacks of either low sensitivity or poor specificity, and even both of them.[6] Consequently, quantitative detection of plasma LPA by optical methods still need complicated sample pretreatment to remove most, if not all, of interfering substances.[6f, 6g] The key bottleneck is the specific recognition of LPA with strong affinity by artificial receptors. On account of the aforementioned low physiological concentrations of LPA, it is highly on demand to design artificial receptors affording extremely strong binding to LPA with exquisite specificity.

Macrocyclic hosts are one family of well-developed artificial receptors with a discrete cavity that is selective for complementary binding to certain guests. With respect to the efficient host-guest interactions between macrocycles and biological substrates in aqueous media, their molecular recognition has gained considerable attention and demonstrated various applications in, but not limited to, the fields of disease diagnosis and therapy, such as sensing of biomarkers,[7] enhancing solubility and stability of drugs,[8] regulating protein-protein interactions,[9] inhibiting amyloid fibril formation.[10] Despite these significant achievements, to our best knowledge, it has never been reported that one macrocycle affords strong binding and specific detection of LPA.

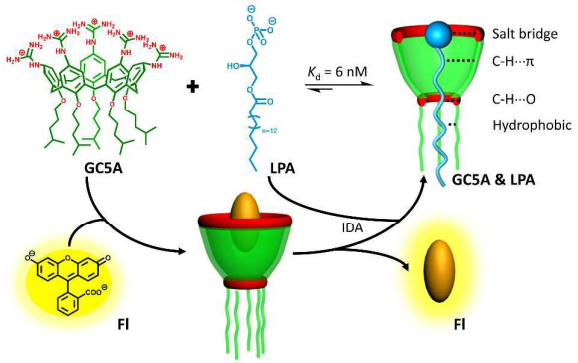

Scheme 1. Schematic illustration of the binding between LPA and GC5A and the operating IDA principle of fluorescence "switch-on" sensing of LPA by the GC5A•Fl reporter pair.

[a] College of Chemistry, State Key Laboratory of Elemento-Organic Chemistry, Key Laboratory of Functional Polymer Materials, Ministry of Education, Nankai University, Tianjin 300071, China. E-mail: dshguo@nankai.edu.cn.
[b] Collaborative Innovation Center of Chemical Science and Engineering, Nankai University, Tianjin 300071, China.

†Electronic Supplementary Information (ESI) available: Experimental details, additional characterisation data. See DOI: 10.1039/x0xx00000x

View Article Online
DOI: 10.1039/C7SC04989G

As a part of our ongoing research exploring biomedical applications by taking advantage of molecular recognition of the calixarene macrocycles,[11] we herein design water-soluble guanidinium-modified calix[5]arene (GC5A), affording the desired strong binding and ultrasensitive fluorescence detection of LPA by means of indicator displacement assay (IDA) in aqueous media (Scheme 1). With respect to the presence of interfering substances and complicated physiological milieu, differential sensing is then introduced to differentiate LPA from all other biologically important species in plasma. More importantly, we achieve the quantitative detection of LPA in the biologically relevant low μM range in serum without any complicated pretreatment procedures, demonstrating its potential for point-of-care testing.

Results and discussion

LPA possesses two potential binding sites: one phosphate head and one long-chain fatty-acid tail. Referring to the structural feature of LPA, we therefore designed the artificial receptor GC5A. First, calixarenes were employed as the macrocyclic scaffold, which have been described as having "(almost) unlimited possibilities" benefiting from their facial modification.[12] Second, among the calix[*n*]arene (C*n*A, *n* = 4, 5, 6, 8 generally) family, we screened C5A on account of size fit. The alkyl chain threads C5A well, but not the smaller C4A, whereas C6A and C8A are relatively larger and have complex conformations.[13] Third, guanidinium groups were decorated at the upper rim of C5A to donate charge-assisted hydrogen bonds (salt bridge) with the phosphate head of LPA.[14] Finally, alkyl chains were attached at the lower rim to provide hydrophobic interaction with the tail of LPA besides rigidifying the C5A conformation. Collectively, these design principles led us to preparing the GC5A host shown in Scheme 1, which is expected to show strong binding to LPA via the synergistic effect among several interactions (electrostatic, hydrogen bond, C–H···π and hydrophobic). The GC5A was prepared mainly according to the syntheses of reported C4A analogues (Scheme 2).[15] In brief, the synthesis started from the maternal *p*-tertbutylcalix[5]arene, which was alkylated at the lower rim to obtain **1** with well-defined cone conformation.[16] Subsequently, **2** was generated by treating **1** with HNO_3 and AcOH to substitute all the *tert*-butyl groups with nitro groups through an *ipso*-nitration reaction. **3** was obtained by reduction of nitro to amino groups by $SnCl_2{\cdot}2H_2O$ in ethanol and ethyl acetate. Then, **4** was obtained by reaction with di-Boc-protected thiourea units. Removal of the protecting groups by stannic chloride finally gave the target GC5A receptor.

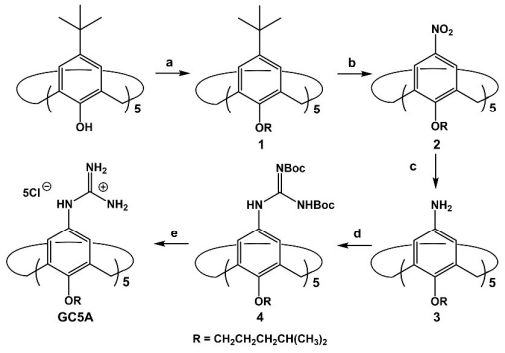

Scheme 2. Synthetic route for GC5A. (a) K_2CO_3, RBr, CH_3CN, reflux, 72%; (b) HNO_3, AcOH, dry CH_2Cl_2, r.t., 46%; (c) $SnCl_2{\cdot}2H_2O$, C_2H_5OH/AcOEt (1:1, v:v), reflux, 52%; (d) N,N'-bis-tert-butoxycarbonylthiourea, Et_3N, $AgNO_3$, dry CH_2Cl_2, r.t., 32%; (e) $SnCl_4$, AcOEt, r.t., 65%.

The GC5A host and the LPA guest are both amphiphilic with critical aggregation concentrations (CACs) of 0.4 and 0.35 mM (Figure S9), respectively.[6h] As a result, measurement of the binding affinity between GC5A and LPA should be implemented at concentrations below their CACs as far as possible to avoid any complication of amphiphilic aggregation. Direct NMR and calorimetric titrations were therefore ruled out since they generally need relatively high concentrations. As an alternative approach, fluorescent IDA that could be operated at low μM or even nM concentrations appears to be a desired choice. IDA, the use of synthetic receptors with competitive binding assays, has been popularized by Anslyn and coworkers as a standard strategy for molecular sensing, complementary to the approach of direct sensing.[7b, 17] We employed IDA to not only determine the binding affinity between GC5A and LPA, but also concurrently offer the opportunity for fluorescence sensing of LPA.

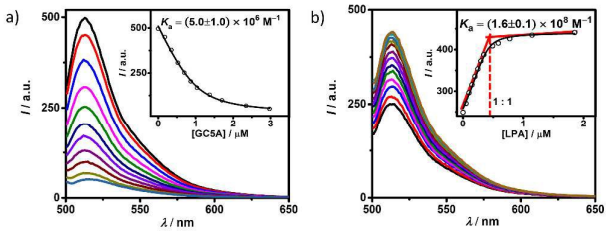

Figure 1. (a) Direct fluorescence titration of Fl (1.0 μM) with GC5A (up to 3.0 μM), λ_{ex} = 500 nm. (Inset) The associated titration curve at λ_{em} = 513 nm and fit according to a 1:1 binding stoichiometry. (b) Competitive titration of GC5A•Fl (0.4/0.5 μM) with LPA (up to 1.9 μM). (Inset) Fit of the titration data to a 1:1 competitive binding model. All experiments are in HEPES buffer (10 mM, pH = 7.4) at 25 °C.

Fluorescein (Fl) was screened as the optimal reporter dye, owing to its high brightness, the strong binding with GC5A and the drastic complexation-induced quenching of fluorescence (Figure 1a). The binding stoichiometry between GC5A and Fl was determined as 1:1 according to the Job's plot (Figure S10). The association constant (K_a) extracted from the fluorescence titration was fitted as $(5.0\pm1.0) \times 10^6$ M^{-1}, which was further validated by the UV-Vis titration (Figure S11). More importantly, the fluorescence depression upon complexation, I_{free}/I_{bound}, is calculated as a factor of 37, which is ideal for the projected IDA application.

The displacement of GC5A•Fl by gradual addition of LPA resulted in regeneration of the intrinsic emission of Fl (Figure 1b). The data was well fitted by the 1:1 competitive binding model, giving the K_a value of $(1.6\pm0.1) \times 10^8$ M^{-1}. The 1:1 binding stoichiometry was clearly verified by the inflection point at 1:1 molar ratio between GC5A and LPA in the competitive titration. To validate the synergistic effect of several interactions on the nanomolar binding between GC5A and LPA, we measured the binding of phosphate and 6:0 LPA (a shorter analogue) with GC5A, giving the K_a values of $(4.6\pm0.6) \times 10^4$ M^{-1} and $(4.8\pm1.0) \times 10^5$ M^{-1} (Figures S12 and S13) respectively. In the case of phosphate, only the salt bridge interaction is presented; in the case of 6:0 LPA, the

View Article Online
DOI: 10.1039/C7SC04989G

hydrophobic interaction between alkyl chains of GC5A and LPA is lacking. So they were merely able to reach the mM to μM binding.

Moreover, two control hosts (GC4A and GC5A-CH_3, see Scheme S3 for their syntheses and structures) were prepared to illustrate the significance of cavity size and rigid cone conformation. The C4A cavity is too small to thread any alkyl chain.[13a] GC4A affords over one order of magnitude weaker affinity ($(1.3\pm0.1) \times 10^5$ M^{-1}) to Fl than GC5A (Figure S14 and S15). By executing IDA, gradual addition of LPA does not lead to pronounced regeneration of the fluorescence in the beginning, indicating the weak complexation of GC4A with LPA (Figure S16). However, in the presence of excess LPA, the fluorescence regenerated. We postulated it is not the *endo*-complexation but the co-assembly between cationic (GC4A) and anionic (LPA) surfactants.[18] The formation of the co-assembly between GC4A and LPA was verified by the dynamic light scattering (DLS) measurements (Figure S17). The scattering intensity increases gradually upon addition of excess LPA, which is in good accordance with the fluorescence result. It is worth noting that no appreciable DLS response was detected for all the direct and competitive titrations of GC5A. Benefiting from the strong host-guest complexation, the titrations were performed at sub-μM concentrations, and no co-assembly was formed. GC5A-CH_3, the control C5A host with conformational flexibility, quenches the fluorescence of Fl to much less extent, and gives the corresponding much weaker affinity ($(4.5\pm0.3) \times 10^4$ M^{-1}) than GC5A (Figure S18). Therefore, both the cavity size and conformational rigidification play crucial roles in the molecular recognition. The employment of C5A, as well as the well-tailored modification, are indispensable to realize the nanomolar binding of GC5A with LPA.

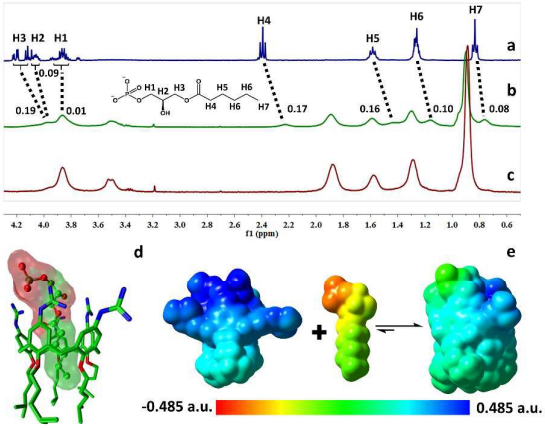

Figure 2. ^{1}H NMR spectra of (a) 6:0 LPA (1 mM), (b) 6:0 LPA (1 mM) with addition of GC5A (1 mM), and (c) GC5A (1 mM) in D_2O at 25 °C. (d) Optimized structure of the GC5A • 6:0 LPA complex at the B3LYP-D3(BJ)/6-31G(d)/SMD(water) level of theory. Hydrogen atoms are omitted for clarity. (e) ESP-mapped molecular vdW surface of GC5A, 6:0 LPA and GC5A•6:0 LPA.

The complexation of LPA with GC5A was further verified by ^{1}H NMR experiments in D_2O. We employed the shorter 6:0 LPA as the model guest for NMR measurements due to the poor water-solubility of the longer LPA species. LPA protons underwent upfield shifts upon addition of GC5A (Figures 2a-c) due to the ring current effect of the aromatic nuclei of calixarenes.[13, 19] It should be mentioned that the complexation-induced shifts of guest protons by GC5A are much less pronounced than those in the other calixarene cases (generally $\Delta\delta$ = 1–2 ppm).[11c, 13a] It arises from the low molecular electrostatic potential of GC5A (*vide infra*) that leading to relatively weak ring current effect. The shifts of H3–H5 signals are larger than the rest, indicating their location in the center of cavity. While H1 and H2 are presumably located at the upper rim, H6 and H7 are close to the lower-rim oxygen mean plane and thread out of the cavity, which are away from the region of maximum shielding provided by the aromatic rings. Moreover, NMR measurements were performed at above CAC, so it is also possible that GC5A and LPA form co-assembly but not *endo*-complex. If GC5A forms co-assembly with LPA possibly, GC4A does too. We further executed the NMR measurements of GC4A with LPA as control, observing no appreciable complexation-induced shift (Figure S20). We therefore deduced that the shifts of LPA protons arose from the *endo*-complexation by GC5A.

Geometry optimization on the GC5A•6:0 LPA complex was performed using the B3LYP-D3(BJ)/6-31G(d)/SMD(water) method.[20] The complex has a threading geometry (Figure 2d), which is in good accordance with the NMR information. To derive further insights for the host-guest binding, we have computed molecular electrostatic potential[21] (ESP) mapped on molecular van der Waal (vdW) surface of GC5A, 6:0 LPA and the GC5A•6:0 LPA complex (Figure 2e). GC5A is very electron-deficient especially at the upper rim, while LPA is electron-rich especially at the phosphate head. The binding mode between GC5A and LPA is favorable because molecules always tend to approach each other in a complementary manner of ESP. Furthermore, the expected hydrogen bonds, C–H···π, C–H···O and vdW interactions between GC5A and LPA were validated by atoms-in-molecules and reduced density gradients analysis (see Supporting Information). Geometry optimization on the GC5A•18:0 LPA complex gives the reasonably consistent results (Figure S30).

The IDA principle based on the GC5A•Fl reporter pair allows for a fluorescence "switch-on" sensing of LPA. As shown in Figure S21, the fluorescence increases linearly with the LPA concentration with good linear performance (R^2 = 0.997). The limit of detection (LOD) for LPA is calculated to be 5.6 nM by utilizing a 3σ/slope method,[22] which is far lower than the requisite detection limit in plasma.[3] Compared with the currently reported fluorescent probes,[6a-c] 5.6 nM represents the lowest LOD value in LPA detection, indicating the ultrahigh sensitivity of GC5A•Fl.

We further tested changes in the fluorescence intensity of GC5A•Fl caused by other biologically important species (nucleoside polyphosphates, amino acids, anions, carbohydrate, ctDNA, RNA and BSA) in plasma to evaluate the sensing selectivity for LPA (Figure 3a). In most cases, the addition of other biological species caused no significant increase in the fluorescence. The only exception was ATP, which resulted in even more pronounced fluorescence response than LPA due to the strong binding of ATP with GC5A (K_a = $(4.7\pm1.4) \times 10^8$ M^{-1}, Figure S24). Such an interference could be easily solved by differential sensing. Differential sensing relies on the composite response of the analyte to the entire array of receptors instead of single receptor, hence also called "array sensing", providing output with better accuracy and more robust interference resistance. Although both the direct sensing and IDA approaches can be used, IDA is more

View Article Online
DOI: 10.1039/C7SC04989G

compatible with differential sensing, because an array can be easily constructed by the combination of multiple receptors and multiple indicators without additional synthetic efforts.[17b] Herein, GC4A was additionally introduced as a receptor, and Al(III) phthalocyanine chloride tetrasulfonic acid ($AlPcS_4$, Scheme S4) was introduced as an additional reporter dye. $AlPcS_4$ is also strongly bound by GC5A and GC4A with drastic fluorescence quenching (Figure S22). We therefore used GC5A•Fl, GC5A•$AlPcS_4$ and GC4A•$AlPcS_4$ as reporter pairs for differential sensing to differentiate LPA from other species in plasma through the different fluorescence response pattern (Figures 3a, 3b and S25). Executing principal component analysis (PCA), an statistical method to find the greatest extents of variance in a set of data, resulted in a score plot (Figure 3c).[23] LPA was definitely distinguished from ATP and the other coexisting species. The major rationale behind the present differential sensing is that the threading complex of LPA could be only formed by GC5A, but not by GC4A. The ratio of fluorescence response (I_{LPA}/I_{ATP}) in the case of GC5A is thus much larger than that in the case of GC4A.

To validate the practically operational detection of LPA, we performed the displacement assay of LPA in mouse serum containing variable LPA concentrations. Despite existing numerous interfering substances in serum, linear increase in the fluorescence of the GC5A•$AlPcS_4$ reporter pair was still observed upon gradually increasing the LPA concentrations (0–80 μM) (Figure 3d). The LOD in serum was calculated as 1.7 μM, which is well below plasma LPA concentrations typically observed in patients with ovarian and other gynecologic cancers. The linear relationship of good performance (R^2 = 0.998) allows us to set up a calibration line of the fluorescence intensity for accurately determining unknown concentrations of LPA down to the low μM range of practical diagnosis relevance. Furthermore, we applied the GC5A•$AlPcS_4$ reporter pair in analyzing cancerous and non-cancerous blood samples.

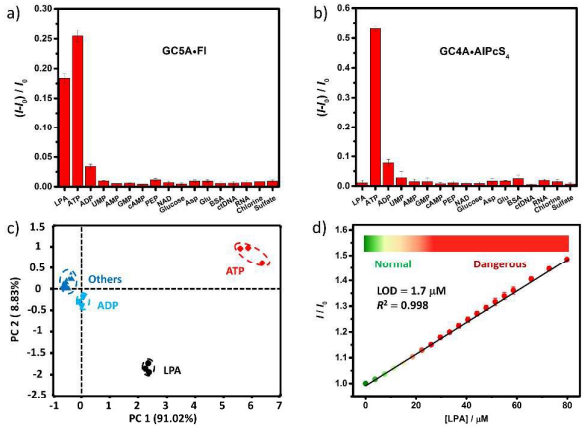

Figure 3. Fluorescence responses of (a) GC5A•Fl (0.8/1.0 μM) at 513 nm (λ_{ex} = 500 nm) (b) GC4A• $AlPcS_4$ (0.8/1.0 μM) at 680 nm (λ_{ex} = 608 nm) upon the addition of LPA and various biologically coexisting species (0.4 μM for small species and 0.15mg/L for ctDNA, RNA and BSA) in HEPES buffer. (c) Score plot of the first two principal components obtained by PCA of analytes. The percent of total variance is given in brackets for each principal component. Ellipsoids on the scatter plot are drawn at 95% confidence. (d) The set-up calibration line of the fluorescence intensity for quantitatively determining the LPA concentrations in serum. Error bars could not be shown if less than 0.005.

The blood samples were obtained from healthy mice and mice with ovarian tumour, which was created by inoculating ID8 cells subcutaneously. Significant difference was observed that the cancerous group gave rise to more fluorescence response than the non-cancerous group (Figure S26). The obtained result validates that the present IDA protocol has great potential in facilitating the practically operational diagnosis of ovarian cancer.

Conclusions

In conclusion, we designed an artificial receptor GC5A for LPA, a cancer biomarker, with the nanomolar affinity in aqueous media. Through IDA coupled with differential sensing, we achieved the ultrasensitive and specific detection of LPA. For accurately determining unknown concentrations of LPA down to the low μM range of practical diagnosis relevance, a calibration line was successfully set up in serum. To the best of our knowledge, although calibration lines of LPA have been obtained among several known assay approaches,[4a, 6f, 6g, 24] the present one represents the first example obtained in untreated serum. These results form the chemistry basis for new protocols and devices to diagnose ovarian cancer and other gynecologic cancers, especially during their early stages.

All animal studies were performed in compliance with the guidelines set by Tianjin Committee of Use and Care of Laboratory Animals and the overall project protocols were approved by the Animal Ethics Committee of Nankai University.

Acknowledgements

This work was supported by NSFC (21672112), the Fundamental Research Funds for the Central Universities and Program of Tianjin Young Talents, which are gratefully acknowledged. We also thank the reviewers' constructive comments.

Notes and references

1. (a) R. C. Bast, B. Hennessy and G. B. Mills, *Nat. Rev. Cancer*, 2009, **9**, 415-428; (b) S. M. Hanash, C. S. Baik and O. Kallioniemi, *Nat. Rev. Clin. Oncol.*, 2011, **8**, 142-150; (c) L. Li, C. W. Zhang, G. Y. Chen, B. Zhu, C. Chai, Q. H. Xu, E. K. Tan, Q. Zhu, K. L. Lim and S. Q. Yao, *Nat Commun.*, 2014, **5**, 3276; (d) L. Zhou, R. Wang, C. Yao, X. Li, C. Wang, X. Zhang, C. Xu, A. Zeng, D. Zhao and F. Zhang, *Nat Commun.*, 2015, **6**, 6938.
2. (a) V. A. Blaho and T. Hla, *Chem. Rev.*, 2011, **111**, 6299-6320; (b) G. B. Mills and W. H. Moolenaar, *Nat. Rev. Cancer*, 2003, **3**, 582-591.
3. Y. Xu, Z. Shen, D. W. Wiper, M. Wu, R. E. Morton, P. Elson, A. W. Kennedy, J. Belinson, M. Markman and G. Casey, *J. Am. Med. Assoc.*, 1998, **280**, 719-723.
4. (a) H. Kim, H. R. Yoon and D. Pyo, *Bull. Korean Chem. Soc.*, 2002, **23**, 1139-1143; (b) Z. Shen, M. Wu, P. Elson, A. W. Kennedy, J. Belinson, G. Casey and Y. Xu, *Gynecol. Oncol.*, 2001, **83**, 25-30; (c) G. Tigyi and R. Miledi, *J. Biol. Chem.*, 1992, **267**, 21360-21367.

View Article Online
DOI: 10.1039/C7SC04989G

5. H. N. Kim, W. X. Ren, J. S. Kim and J. Yoon, *Chem. Soc. Rev.*, 2012, **41**, 3210-3244.
6. (a) M. H. Lan, W. M. Liu, Y. Wang, J. C. Ge, J. S. Wu, H. Y. Zhang, J. H. Chen, W. J. Zhang and P. F. Wang, *ACS Appl. Mater. Interfaces*, 2013, **5**, 2283-2288; (b) D. F. Yao, Z. Lin and J. C. Wu, *ACS Appl. Mater. Interfaces*, 2016, **8**, 5847-5856; (c) W. W. Zhao, W. M. Liu, W. J. Zhang, L. T. Zeng, Z. Y. Fan, J. S. Wu and P. F. Wang, *Analyst*, 2012, **137**, 1853-1859; (d) L. Wang, M. Sibrian-Vazquez, J. O. Escobedo, J. Wang, R. G. Moore and R. M. Strongin, *Chem. Commun.*, 2015, **51**, 1697-1700; (e) S.-Y. Zhang, W. Shi, P. Cheng and M. J. Zaworotko, *J. Am. Chem. Soc.*, 2015, **137**, 12203-12206; (f) O. Alpturk, O. Rusin, S. O. Fakayode, W. Wang, J. O. Escobedo, I. M. Warner, W. E. Crowe, V. Kral, J. M. Pruet and R. M. Strongin, *Proc. Natl. Acad. Sci. USA*, 2006, **103**, 9756-9760; (g) T. Jiang, N. Lu, J. Yang, Y. Hang, J. Wang, P. Zhao and J. Hua, *RSC Adv.*, 2015, **5**, 102863-102867; (h) K. H. Chen, J. S. Yang, C. Y. Hwang and J. M. Fang, *Org. Lett.*, 2008, **10**, 4401-4404.
7. (a) G. Ghale and W. M. Nau, *Acc. Chem. Res.*, 2014, **47**, 2150-2159; (b) B. T. Nguyen and E. V. Anslyn, *Coord. Chem. Rev.*, 2006, **250**, 3118-3127; (c) B. J. Shorthill, C. T. Avetta and T. E. Glass, *J. Am. Chem. Soc.*, 2004, **126**, 12732-12733; (d) P. Sokkalingam, D. S. Kim, H. Hwang, J. L. Sessler and C.-H. Lee, *Chem. Sci.*, 2012, **3**, 1819-1824; (e) J. Ma, Q. Meng, X. Hu, B. Li, S. Ma, B. Hu, J. Li, X. Jia and C. Li, *Org. Lett.*, 2016, **18**, 5740-5743.
8. (a) I. Ghosh and W. M. Nau, *Adv. Drug Delivery Rev.*, 2012, **64**, 764-783; (b) G. Ping, Y. Wang, L. Shen, Y. Wang, X. Hu, J. Chen, B. Hu, L. Cui, Q. Meng and C. Li, *Chem. Commun.*, 2017, **53**, 7381-7384; (c) B. Li, Z. Meng, Q. Li, X. Huang, Z. Kang, H. Dong, J. Chen, J. Sun, Y. Dong, J. Li, X. Jia, J. L. Sessler, Q. Meng and C. Li, *Chem. Sci.*, 2017, **8**, 4458-4464; (d) S. Liu, D. H. Russell, N. F. Zinnel and B. C. Gibb, *J. Am. Chem. Soc.*, 2013, **135**, 4314-4324; (e) A. I. Lazar, F. Biedermann, K. R. Mustafina, K. I. Assaf, A. Hennig and W. M. Nau, *J. Am. Chem. Soc.*, 2016, **138**, 13022-13029.
9. (a) K. D. Daze, T. Pinter, C. S. Beshara, A. Ibraheem, S. A. Minaker, M. C. F. Ma, R. J. M. Courtemanche, R. E. Campbell and F. Hof, *Chem. Sci.*, 2012, **3**, 2695-2699; (b) R. E. McGovern, H. Fernandes, A. R. Khan, N. P. Power and P. B. Crowley, *Nat. Chem.*, 2012, **4**, 527-533.
10. (a) H. H. Lee, T. S. Choi, S. J. C. Lee, J. W. Lee, J. Park, Y. H. Ko, W. J. Kim, K. Kim and H. I. Kim, *Angew. Chem., Int. Ed.*, 2014, **53**, 7461-7465; (b) M. N. Shinde, N. Barooah, A. C. Bhasikuttan and J. Mohanty, *Chem. Commun.*, 2016, **52**, 2992-2995.
11. (a) D.-S. Guo and Y. Liu, *Acc. Chem. Res.*, 2014, **47**, 1925-1934; (b) D.-S. Guo, J. Yang and Y. Liu, *Chem. Eur. J.*, 2013, **19**, 8755-8759; (c) D.-S. Guo, V. D. Uzunova, X. Su, Y. Liu and W. M. Nau, *Chem. Sci.*, 2011, **2**, 1722-1734; (d) D.-S. Guo, K. Wang, Y.-X. Wang and Y. Liu, *J. Am. Chem. Soc.*, 2012, **134**, 10244-10250.
12. V. Böhmer, *Angew. Chem., Int. Ed.*, 1995, **34**, 713-745.
13. (a) M. De Rosa, C. Talotta, C. Gaeta, A. Soriente, P. Neri, S. Pappalardo, G. Gattuso, A. Notti, M. F. Parisi and I. Pisagatti, *J. Org. Chem.*, 2017, **82**, 5162-5168; (b) G. Gattuso, A. Notti, S. Pappalardo, M. F. Parisi, I. Pisagatti and S. Patanè, *New J. Chem.*, 2014, **38**, 5983-5990.
14. (a) S. L. Tobey and E. V. Anslyn, *J. Am. Chem. Soc.*, 2003, **125**, 14807-14815; (b) W.-C. Geng, Y.-C. Liu, Y.-Y. Wang, Z. Xu, Z. Zheng, C.-B. Yang and D.-S. Guo, *Chem. Commun.*, 2016, **53**, 392-395.
15. F. Sansone, M. Dudic, G. Donofrio, C. Rivetti, L. Baldini, A. Casnati, S. Cellai and R. Ungaro, *J. Am. Chem. Soc.*, 2006, **128**, 14528-14536.
16. F. Arnaud-Neu, S. Fuangswasdi, A. Notti, S. Pappalardo and M. F. Parisi, *Angew. Chem., Int. Ed.*, 1998, **37**, 112-114.
17. (a) A. E. Hargrove, S. Nieto, T. Zhang, J. L. Sessler and E. V. Anslyn, *Chem. Rev.*, 2011, **111**, 6603-6782; (b) L. You, D. Zha and E. V. Anslyn, *Chem. Rev.*, 2015, **115**, 7840-7892; (c) S. L. Wiskur, H. Ait-Haddou, J. J. Lavigne and E. V. Anslyn, *Acc. Chem. Res.*, 2001, **34**, 963-972.
18. Y. Yan and J. Huang, *Coord. Chem. Rev.*, 2010, **254**, 1072-1080.
19. D.-S. Guo, H.-Q. Zhang, F. Ding and Y. Liu, *Org. Biomol. Chem.*, 2012, **10**, 1527-1536.
20. (a) P. J. Stephens, F. J. Devlin, C. F. Chabalowski and M. J. Frisch, *J. Phys. Chem.*, 1994, **98**, 11623-11627; (b) A. D. Becke, *J. Chem. Phys.*, 1993, **98**, 5648-5652; (c) P. C. Hariharan and J. A. Pople, *Theor. Chim. Acta.*, 1973, **28**, 213-222; (d) W. J. Hehre, R. Ditchfield and J. A. Pople, *J. Chem. Phys.*, 1972, **56**, 2257-2261.
21. J. S. Murray and P. Politzer, *WIREs Comput. Mol. Sci.*, 2011, **1**, 153-163.
22. (a) G. B. Huang, S. H. Wang, H. Ke, L. P. Yang and W. Jiang, *J. Am. Chem. Soc.*, 2016, **138**, 14550-14553; (b) D. MacDougall and W. B. Crummett, *Anal. Chem.*, 2002, **52**, 2242-2249.
23. S. Stewart, M. A. Ivy and E. V. Anslyn, *Chem. Soc. Rev.*, 2014, **43**, 70-84.
24. Y. Wang, H. Pei, Y. Jia, J. Liu, Z. Li, K. Ai, Z. Lu and L. Lu, *J. Am. Chem. Soc.*, 2017, **139**, 11616-11621.

View Article Online
DOI: 10.1039/C7SC04989G

Table of contents entry

for

Ultrasensitive and Specific Fluorescence Detection of a Cancer Biomarker via Nanomolar Binding to a Guanidinium-modified Calixarene

Zhe Zheng,[a] Wen-Chao Geng,[a] Jie Gao,[a] Yu-Ying Wang,[a] Hongwei Sun,[a] and Dong-Sheng Guo*[a,b]

[a]College of Chemistry, State Key Laboratory of Elemento-Organic Chemistry, Key Laboratory of Functional Polymer Materials, Ministry of Education, Nankai University, Tianjin 300071, China. E-mail: dshguo@nankai.edu.cn.
[b]Collaborative Innovation Center of Chemical Science and Engineering, Nankai University, Tianjin 300071, China.

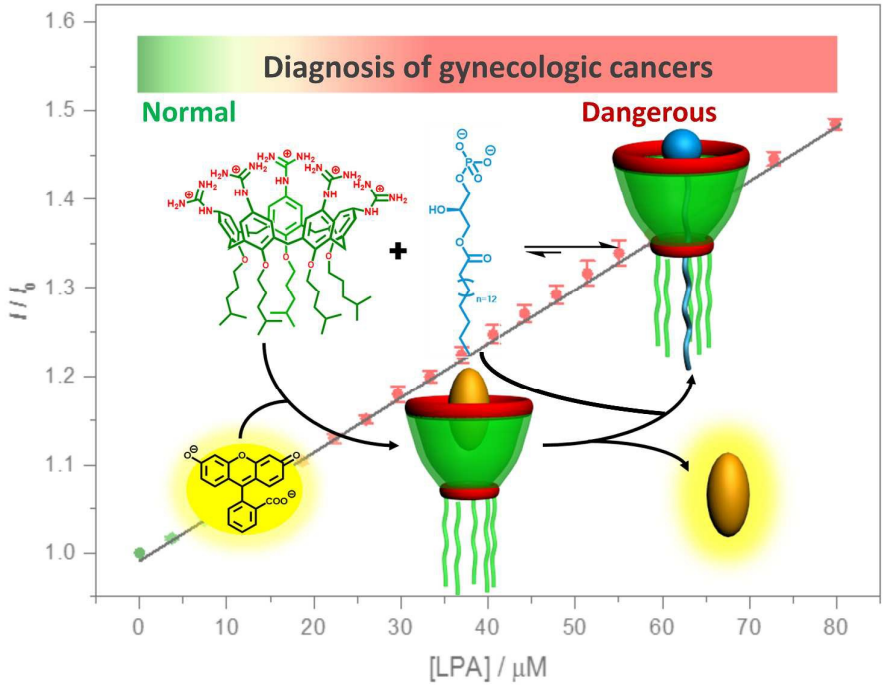

A well-designed macrocycle affords nanomolar binding to a cancer biomarker lysophosphatidic acid, showing potential application in diagnosis of gynecologic cancers.